RSC Advances

Accepted Manuscript
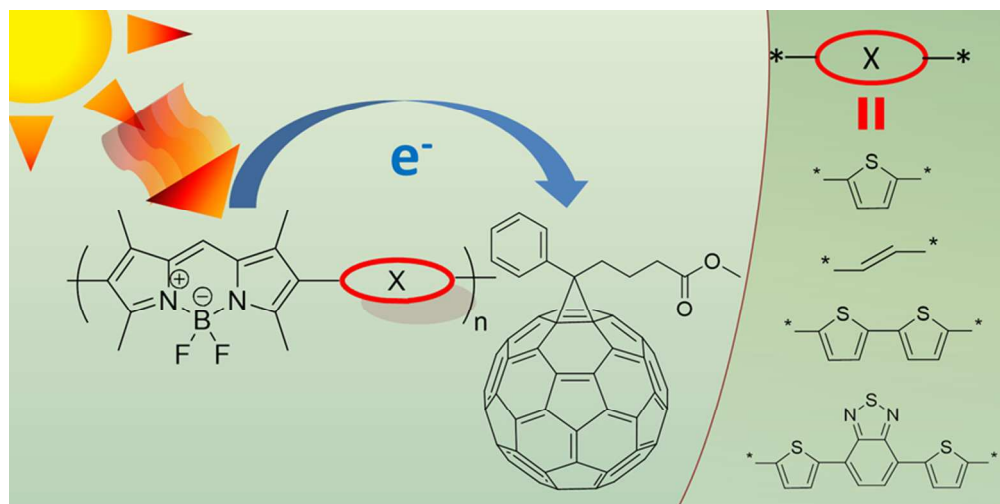
RSCPublishing

A series of conjugated polymers donors based on the BODIPY moiety have been synthesized and characterized aiming at polymer: fullerene solar cells applications
80x39mm (300 x 300 DPI)

ARTICLE TYPE

Novel BODIPY-based Conjugated Polymers Donors for Organic Photovoltaic Applications

Solon P. Economopoulos,[a] Christos L. Chochos,[a] Heraklidia A. Ioannidou,[b] Marios Neophytou,[a] Charilaos Charilaou,[e] Georgia A. Zissimou,[b] Jarvist Moore Frost,[c] Tuladhar Sachetan,[c] Munazza
[5] **Shahid,[d] Jenny Nelson,[c] Martin Heeney,[d] Donal D. C. Bradley,[c] Grigorios Itskos,[e] Panayiotis A. Koutentis,[b] and Stelios A. Choulis*[a]**

[10] Five new polymers based on the 4,4-difluoro-4-bora-3*a*,4*a*-diaza-*s*-indacene core (**BODIPY**) chromophore moiety have been synthesized as low bandgap polymers for optoelectronic applications. The polymers exhibited high solubility in common organic solvents and optical bandgaps ranging from 1.7-2 eV. The materials were characterized using NMR, UV-Vis, steady state and time-resolved photoluminescence and the energy levels were examined using electrochemistry and validated using
[15] quantum chemical calculations. Finally, a representative **BODIPY** derivative**:PCBM** blend was examined in terms of photovoltaic properties. Preliminary device performance parameters as a function of photo-active layer thickness and composition are reported and discussed, relating to power convesion efficiency values.

Introduction

[20] A decade ago, polymer:fullerene solar cells were barely hitting the 1% efficiency milestone.[1] A deep understanding of underlying physics in these systems[2-4] through the use of reliable reference compounds in the form of phenylene-vinylene[5] and thiophene[6] polymeric analogues helped
[25] efficiencies reach 5%.[7] However, during the last 6 years it has become clear that the road towards high power conversion efficiency solar cells, will require new materials. Powered by novel conjugated polymer architectures, efficiencies have now almost doubled and are nearing the 10% mark.[8] Theoretical[9]
[30] and experimental[10] approaches towards obtaining high performance materials have been documented, and the state of the art today includes polymers based on benzo[1,2-*b*:4,5-*b*']dithiophenes,[11-15] Si[16] or Ge[17] bridged cyclopentadithiophenes, and carbazoles.[18]
[35] 4,4′-Difluoro-4-bora-3a,4a-diaza-*s*-indacenes (**BODIPY**) dyes have recently attracted considerable attention owing mainly to their interesting optical properties. Numerous reports on **BODIPY** molecules have emerged describing their chemistry.[19-22] Despite being introduced a few years ago, a
[40] large number of donor-acceptor hybrids have already been prepared, either with fullerenes[23-29] or with other molecular electron acceptors,[30] which is a testament to their interest and potential. While several **BODIPY** small organic molecules have been synthesized and explored towards their
[45] photovoltaic capabilities[31-34] conjugated polymers incorporating the **BODIPY** moiety are still scarce[35-39] and

reports on solar cells with bodipy-based conjugated polymers as the electron donor yield relatively low efficiencies.[40-42] Herein, we present the synthesis and characterization of one
[50] **BODIPY** homopolymer and four new copolymers with various groups complementing the **BODIPY** dye central moiety. The materials have been characterized structurally and optically. Since the goal is to provide conjugated polymers, suitable for light harvesting in polymer fullerene solar cells, electrochemical
[55] and computational studies were carried out to provide insight on the energy levels of these new materials and to validate the computational design method. Preliminary solar cell device performance data are also presented.

Results and Discussion

[60] 2,6-Dibromo-4-hexyl-1,3,5,7-tetramethylborondipyrro-methene **3** was synthesized as outlined in Scheme 1. Condensation of 2,4-dimethylpyrrole with heptanoyl chloride provided the dipyrromethene monomer **1**, which on treatment with trifluoroborane dietherate and diisopropylethylamine (Hünig's
[65] base) gave the borondipyrromethene monomer **2** in 54% overall yield. Bromination of the borondipyrromethene at the 2- and 6-positions using molecular bromine gave the corresponding 2,6-dibromo-4-hexyl-1,3,5,7-tetramethylborondipyrromethene **3** in over 50% yield.
[70] Stille cross-coupling polymerization using 1:1 monomer feed ratios were used to prepare the polymers. In a typical experiment, to a solution of 2,6-dibromo-4-hexyl-1,3,5,7-tetramethylboron-dipyrromethene **3** in dry deoxygenated toluene was added the

RSC Advances Accepted Manuscript

corresponding distannyl arenes (1 equiv.) in the presence of tris(dibenzylideneacetone)dipalladium(0) [$Pd_2(dba)_3$] (2 mol %) and tri-*o*-tolylphosphine [(*o*-Tol)$_3$P] (8 mol %) and the mixture was heated to *ca.* 110 °C for 24 h to give after work up the corresponding polymers (Scheme 2). The typical work up involved precipitation of the reaction mixture into methanol, subsequent filtration and drying *in vacuo*. The isolated solids were then purified by Soxhlet extraction with methanol (200 mL, 1 d), hexane (200 mL, 1 d) and chloroform (200 mL, 1 d). The chloroform fraction was then concentrated under reduced pressure, precipitated in methanol, filtered and dried *in vacuo*. The resulting polymers were readily soluble in chloroform, chlorobenzene and *o*-dichlorobenzene (o-DCB).

The polymers were characterized with ^{1}H NMR spectroscopy and gel permeation chromatography (GPC) [see Supporting Information for NMR assignments and GPC chromatograms (Figure S8]. The typical molecular weights (MW) of the polymers and polydispersities were estimated by GPC (Table 1).

Optical Properties

The optical properties of the monomers and polymers were studied using absorption and fluorescence spectroscopy. Data obtained from optical measurements in solutions and thin films are summarized in Table 2. The steady-state absorption spectra of monomers **2** and **3** in solution are similar to other known borondipyrromethene derivatives[43] with absorption maxima at 499 and 525 nm, respectively (Table 2, Fig. S10). The polymers in solution exhibit longer wavelength absorption compared to the monomers and relatively large Stokes shifts (0.3-0.4 eV), except the **PB** homopolymer, indicating a high energetic relaxation of photoexcitations, in the copolymers, before radiative recombination.

The optical characteristics of the films, are shown in Fig. 1, where absorption and emission spectra of the synthesized materials are presented. The main films absorption band, with the exception of **PBE**, is centered at 570-580 nm. The ethylene-containing **PBE** shows a small bathochromic-shift of 10-20 nm that can be attributed to slightly stronger π-π interactions caused by the vinyl groups higher delocalization compared to the aromatics.[44]

The optical bandgaps for the bodipy polymers are comparable to those of established light harvesting polymers such as alternating polyfluorenes (**APFO3**)[45] and Poly[[9-(1-octylnonyl)-9H-carbazole-2,7-diyl]-2,5-thiophenediyl-2,1,3-benzothiadiazole-4,7-diyl-2,5-thiophenediyl] (**PCDTBT**),[46] showing that borondipyrromethene can be a viable alternative as a building block to the widely-used fluorene and carbazole moieties. Under resonant excitation at the peak of their absorption bands the films exhibit strong and featureless fluorescence with maxima ranging from 700 to 720 nm (Fig. 1-bottom) with the exception of **PB** and **PBE** that shows weaker, red-shifted emission up to 735 nm. Time-resolved photoluminescence experiments were carried out on the polymer **PBTT** which exhibited the highest absorption coefficient in thin film form as well as on the **PBT** in order to examine whether the addition of the thiophene moiety influences the exciton lifetime. Polymers in pristine form and in blends with **PCBM** were excited by a 375 nm (3.31 eV) ps laser using a spectrometer-based Time-Correlated Single Photon Counting

(TCSPC) system (~150 ps time resolution after reconvolution with the instrument response function). The decays at the fluorescence peaks of the **PBT** and **PBTT** films and their respective blends with **PCBM** are shown in logarithmic scale, along with the instrument response function in Figure 2.

An efficient quenching of the PL lifetime is observed in both blend films relative to that of the pristine materials. Reconvolution using the DAS6 (Horiba Jobin Yvon) software analysis package reveals that pristine materials exhibit biexponential decays with an effective lifetime of of 264 ps for **PBT** and 275 ps for **PBTT** while the blend excitations decay visibly faster. The efficient quenching of the PL lifetime can be predominantly attributed to polymer exciton dissociation due to interfacial electron transfer from to the **PCBM.** The two blends with fullerene exhibit similar fluorescence kinetics and similar values of lifetime quenching. The latter can be viewed as a measure of the exciton dissociation efficiency due to electron transfer from the polymers to the **PCBM**. However, a fraction of the blend excitations potentially decay at timescales faster than the instrument resolution (~150 ps). The data from the lifetime measurements are summarized in Table 3.

Electrochemical characterization

All the materials were studied by electrochemistry. All the voltammograms are presented in Figure 3, while the data are summarized in Table 2. Aside from cyclic voltammetry (CV), differential pulse voltammetry (DPV) was used due to the higher sensitivity of the technique and for measurements less influenced by capacitive current. As a general observation all films were extremely sensitive to the application of current.

Upon examination of the parent molecule **3**, in solution (DCM) a reversible reduction was observed, attributed to the BODIPY moiety,[47] at -1.76 V and an irreversible oxidation at 0.74 V. The resulting HOMO and LUMO values from the onsets, yield 5.61 and 3.41 eV, respectively. The electrochemical bandgap, was in excellent agreement with the optical bandgap, found from the absorption spectra. On examination of the polymers in thin film, the CV of polymer **PB** gave a broad quasi reversible reduction at -1.63 V affording a LUMO value of 3.77 eV. Examination using either CV, or DPV, could not reveal an oxidation process. By using the LUMO value of 3.77 eV and the optical bandgap of 1.97 eV, a HOMO of around 5.74 eV was calculated. By comparison to the monomer **3**, the polymerization, yields a homopolymer with deeper HOMO and LUMO levels. Examination of **PBT** reveals two reversible processes, an oxidation at 0.74 V and a reduction at -1.54 V. These values represent HOMO and LUMO levels of 5.63 and 3.58 eV, respectively. The electrochemical bandgap is in fairly good agreement with the optical bandgap, (as is the case with all the examined polymers) with a discrepancy of 0.18 eV. The same trend is seen with the rest of the polymers. LUMO values remain at levels of around 3.6-3.8 eV in good agreement with other BODIPY copolymers[41] and considerably reduced when compared to the parent molecule **3**. As a comparison note, **PCBM** was also examined and found to exhibit a LUMO value of 4.08 eV (not shown) so charge transfer from the **BODIPY** conjugated polymers to fullerene adducts, should be, energetically, favored. Additional confirmation of the

thermodynamically favorable charge transfer can come from employing the Rehm-Weller equation where a $\Delta G = E^0_{D+/D} - E^0_{A/A-} - E_g + C$ where $E^0_{D+/D}$ is the oxidation (vs SCE) of the **PBT** donor, $E^0_{A/A-}$ the reduction (vs SCE) of the **PCBM** acceptor,

5 E_g the bandgap of the polymer and C the Coulombic interaction (0.06 eV for acetonitrile). A ΔG value of -0.28 eV is calculated, thermodynamically enabling complex formation of the polymer with the fullerene. Comparing **PBT** and **PBTT**, there is a slight lowering of the LUMO at 3.76 eV, and a second oxidation peak is

10 seen at 1.06 V, possibly attributed to a stronger thiophene character present in the end-material. In copolymer **PBTBT** two reversible reductions overlapping with each other at -1.51 and -1.70 V are evident. The first is attributed to the benzothiazole moiety (Fig. S11) and the latter is attributed to the **BODIPY**

15 moiety. The energy levels extracted from this series of materials are in good accord with those of polymers with much higher MW.[40, 48] The low molecular weights, obtained, do not factor-in considerably, so as to preventing any meaningful extraction of trends. This denotes that the materials synthesized possess an

20 adequate effective conjugation length to allow for electrochemical alterations, compared to the parent molecule.

Computational Studies

Following a methodology previous developed with functionalised fullerene acceptors,[49] HOMO and LUMO energy levels were

25 estimated for these materials by combined hybrid DFT and TD-DFT (B3LYP/6-31g*) calculations on dimers. Due to the very different environments of calculation vs experiment (isolated molecules in vacuum vs dense films in solvent) it is not possible to directly compare quantities, but qualitative trends in the energy

30 levels are of interest. Calculations were made for oligomers of **PBE**, **PBT** and **PBTBT** and the data are summarized in Table 4. The qualitative trend calculated, in going from **PBE** to **PBT**, of a slight deepening of the HOMO energy is reflected in the cyclic-voltammetry measurements. However, the prediction of a more

35 shallow HOMO and smaller bandgap for **PBTBT** disagrees with experiment. We attribute this discrepancy to the highly charge-transfer nature of benzothiazole (**BT**) containing donor-acceptor materials leading to misprediction by hybrid DFT.

Photovoltaic Performance

40 An attempt to probe the photovoltaic properties of the synthesized polymers was carried out. As such, **PBT** and **P3HT**, which have similar optical absorption coefficients, were compared. A hole transporting polymer, **PEDOT:PSS**, was spin coated on top of pre sputtered ITO substrates in standard device

45 configuration (see Experimental Section). Organic bulk heterojunction solar solar cells were fabricated with different composition ratios of **PBT** and **PCBM**. Materials were separately diluted in chlorobenzene and stirred overnight at 70 °C with an overall concentration set to 30 mg/mL. Solutions were mixed one

50 hour prior to deposition at different spin rates. Figure 4 summarizes main device parameters with respect to thickness and weight ratio of **PCBM** in the **PBT** conjugated polymer. In common with blend devices made from other amorphous conjugated polymers with PCBM, the current density and Fill

55 Factor (FF) increases with fullerene content reaching a maximum at 75 − 80 wt. %. As expected, relatively constant open circuit

voltage (Voc) values were observed as a function of weight ratio of **PCBM** in the PBT conjugated polymer.

As the **PBT** copolymer possesses comparable absorption

60 coefficient to **P3HT**, it makes sense to examine one of the main bottlenecks for highly efficient **BODIPY** polymer-based solar cells, the low charge carrier mobilities. We conducted a basic thickness dependence of device performance, aiming at elucidating whether thinner layers will improve on performance,

65 should the main reason for low power conversion efficiencies lies in low carrier mobility. By varying the spin rate, 65, 80 and 120 nm of optically active layers were obtained. Thicker devices regardless of the composition ratio exhibited FF values below 25%, the theoretical minimum. As shown from Figure 4b at +1 V

70 the photovoltaic device performance is dominated by series resistance and noncontiguous pathways seem to be the most logical explanation. Summarizing, for the selected BODYPI derivative under study (PBT) optimum overall device performance was achieved with optically active layer in the range

75 of ~65 nm with 75 wt % of **PCBM**. Power conversion efficiency (PCE) of 0.62% with Jsc 2.65 mA/cm^2, Voc 883 mV and FF values of 26.3% were obtained. Concerning the state of the art in BODIPY-based polymers of ~2%,[40] it is evident that there is a large headroom for optimization of the device performance, but

80 these preliminary results provide valuable information on the direction of future device processing conditions.

Conclusion

Five new **BODIPY**-based polymers were synthesized and characterized. Despite moderate molecular weights, the optical

85 measurements revealed that **BODIPY** moiety can be a viable alternative to base synthetic efforts for solar harvesting polymers. An efficient quenching of the PL lifetime is observed in **BODIPY**:**PCBM** blends relative to that of the pristine conjugated polymers, indicating the presence of a fast exciton dissociation

90 at the **BODIPY**:**PCBM** heterointerfaces. Electrochemical measurements showed good agreement of the electrochemical and optical bandgaps and good energy level matching with **PCBM** as well as ITO/PEDOT:PSS and justified the inspiring open circuit voltage values obtained. Preliminary organic solar

95 cell device performance for a representative **BODIPY** derivative (**PBT**) with absorption coefficient similar to **P3HT** was studied as a function of active layer thickness and **PCBM** weight ratio. Representative **PBT**:**PCBM** (1:4) weight ratio based bulk heterojunction organic solar cells confirmed the high open circuit

100 voltage (Voc) values for this material system (Voc=883 mV) and showed PCE of 0.62% due to low FF and Jsc values. However the **PBTT** and **PBE** conjugated polymers presented, display significantly high absorption coefficient in comparison to **P3HT** and show potential for higher PCE values. A comprehensive

105 study including transport, morphology and device performance optimisation study for all the synthesized **BODIPY** conjugated polymers presented are currently underway.

Experimental Procedure

Instrumentation

Melting points were determined using a TA Instruments DSC Q1000 with samples hermetically sealed in aluminium pans under an argon atmosphere; using heating rates of 5 °C/min, and are defined by their onset and peak temperatures. ^{1}H NMR spectra

[5] were recorded on a Bruker Avance 500 machine at 500 MHz. Deuterated solvents were used for homonuclear lock and the signals are referenced to the deuterated solvent peaks. MALDI-TOF MS were conducted on a Bruker BIFLEX III time-of-flight (TOF) mass spectrometer. Microanalysis was performed

[10] at London Metropolitan University on a Perkin Elmer 2400 Series II CHN Analyzer.

Film absorption was carried out at a Lambda 1050 UV/Vis/NIR spectrophotometer (Perkin Elmer). For absorption coefficient measurements the polymer films were measured as per the film

[15] thickness using a Veeco DEKTAK 150 profilometer and results were calibrated in order to eliminate differences in film thickness. Steady-state and time-resolved fluorescence were measured on a NanoLog FL3 spectrofluorometer (Horiba Jobin Yvon). Steady-state spectra were excited by an Ozone-free 450W Xenon Lamp.

[20] Time-resolved fluorescence was measured by the time-correlated single-photon counting (TCSPC) method using a picosecond laser diode as an excitation source (NanoLED, 375 nm). The decays curves were recorded at 700 nm within a narrow spectral window of ± 2 nm. The wavelength was chosen so as to be in the

[25] vicinity of the polymers peak fluorescence i.e. 696 nm for PBTT and 716 nm for PBT and to avoid any appreciable interference from the excited PCBM from the 375 nm excitation laser source. The system exhibits a time-resolution of ~150 ps after reconvolution with the laser excitation pulses using the DAS6

[30] (Horiba Jobin Yvon) software analysis package.

Number-average (Mn) and weight-average (Mw) were determined by Agilent Technologies 1200 series GPC running in chlorobenzene at 80 °C, using two PL mixed B columns in series, and calibrated against narrow polydispersity polystyrene

[35] standards.

Electrochemistry studies were performed using a standard three-electrode cell under argon atmosphere. All measurements were performed with Ar bubbling into the electrochemical cell for 15 min. 10 sec prior to the measurements, the Ar was turned to

[40] "blanket-mode". Platinum wire (99.99%) was used as working electrode and platinum gauze (55 mesh, 99.9%) as counter electrode. Silver/silver chloride was used as a reference electrode. Tetrabutylammonium hexafluorophosphate (TBAPF$_6$, 98%) was used as electrolyte and was recrystallized three times from

[45] acetone and dried in vacuum at *ca* 100 °C before each experiment. Measurements were recorded using an EG&G Princeton Applied Research potensiostat/galvanostat Model Verstastat 4 connected to a personal computer running VersaStudio software. The scan rate was kept constant for all CV

[50] runs at 100 mV/s while for differential pulse voltammetry measurements, the following parameters were used Step height: 25 mV, Step Width: 5 mV, Pulse height: 50 ms, Pulse Width: 100 ms. All results were calibrated using commercially available ferrocene (purified by sublimation) as internal standard. All

[55] polymer samples were studied in solid state by forming a thin film on the working electrode from a viscous DCM solution of the polymer and subsequent drying of the electrode. To calculate HOMO/LUMO levels, using the potentials obtained the following equations[50] were used

[60] $E_{HOMO} = - (E[ox \, vs \, Fc/Fc^+] + 5.1) \, (eV)$

$E_{LUMO} = - (E \, [red \, vs \, Fc/Fc^+] + 5.1) \, (eV)$

For HOMO-LUMO estimations, the onset of the peak was considered.

Computational studies

[65] Calculations estimated the HOMO energy from the energy of the highest occupied Kohn-Sham orbital of a ground state B3LYP hybrid-density functional theory calculation with a 6-31g* basis set (also used for geometry optimisation). The LUMO was estimated by combining this energy with the first Singlet

[70] excitation energy as calculated by linear response time-dependent density functional theory with the same basis and functional. Quantum chemical (QC) calculations used the Gaussian09 [51] software package, and were undertaken at the Imperial College High Performance Computing Service.[52] From the data obtained

[75] the calculated 1st singlet and the experimental Eg values are the ones that should be compared.

Devices and characterization

The devices based on **PBT** (**BODIPY** derivative)**:PCBM** active layer and **PEDOT:PSS** buffer layer were processed in

[80] ambient atmosphere, in the state-of-the-art clean room facilities at Imperial College. Pre-patterned ITO coated glass substrates (obtained from PsioTech) were cleaned in acetone, DI water and isopropanol in an ultrasonic bath for 15 min. Subsequently ITO substrates were dried and treated with oxygen plasma before

[85] coating with **PEDOT:PSS** (~40nm) as a hole extraction layer. The samples were baked on a hot plate at 150 °C for 20 min. The various **BODIPY:PCBM** blends (30mg/mL) in chlorobenzene solvents are deposited onto substrates by spin coating process. The device structure was then completed with the evaporation of

[90] ~10 nm of Ca and ~100 nm thick Al top electrode by thermal evaporation under 10^{-6} Torr using a shadow mask. The area of a single device was ~4.5 mm^2. The current- voltage (J-V) characteristics of the devices were measured with a Keithley 2400 source meter by illuminating through the semitransparent

[95] ITO electrode with simulated solar irradiance (AM 1.5G) light from a filtered Xe lamp at an intensity of 100 mW/cm^2. The calibration of the incident light was performed with a silicone photodiode (RS BPW21). The thickness of all the sample films was measured by an alpha-step profiler.

[100] ### Materials

All solvents and reagents were purchased from Aldrich and were used without further purification, unless otherwise stated.* Column chromatography was performed on silica gel (Merck TLC-Kieselgel 60H, 15 lm)

[105] ### Monomer and Polymer Synthesis

*(Z)-2-[1-(3,5-Dimethyl-2*H-*pyrrol-2-ylidene)heptyl]-3,5-dimethyl-1*H-*pyrrole hydrochloride* (**1**). To a stirred solution of 2,4-dimethylpyrrole (2.7mL, 26.3 mmol) in DCM (20 mL) was added dropwise over a period of 15 min n-heptanoyl chloride

[110] (9.44 mL, 61.3 mmol). The reaction mixture was then heated at *ca*. 40 °C for 4 h and then allowed to cool to *ca*. 20 °C. The

solvent was removed *in vacuo* to give the crude monomer **1** (8.2 g, 97%) which was used in the next step without any further purification.

*5,5-Difluoro-10-hexyl-1,3,7,9-tetramethyl-5*H-*dipyrrolo[1,2-*
5 c*:2',1'-*f*][1,3,2]diazaborinin-4-ium-5-uide* (**2**). To a solution of the crude (*Z*)-2-[1-(3,5-dimethyl-2*H*-pyrrol-2-ylidene)heptyl]-3,5-dimethyl-1*H*-pyrrole hydrochloride (**1**) (8.2 g, 25.6 mmol) in toluene (200 mL) at *ca.* 20 °C was added Hünig's base (21 mL, 120 mmol) and the mixture was stirred for 1.5 h. Under
10 continuous stirring, was added dropwise boron trifluoride etherate (22 mL, 175 mmol) affording a green fluorescence. The reaction mixture was then heated at *ca.* 80 °C for 1 h, and then allowed to cool to *ca.* 40 °C, washed with warm water (3 × 100 mL), dried (MgSO$_4$) and concentrated to give a dark brown solid. Column
15 chromatography [hexane → hexane/toluene (1:4)] gave the *title compound* **2** as orange needles (2.51 g; overall yield: 54%), mp (DSC) onset: 111.3 ^{o}C, peak: 112.2 ^{o}C (MeOH); found: C, 68.73; H, 8.30; N, 8.49. C$_{19}$H$_{27}$BF$_2$N$_2$ requires 68.69; H, 8.19; N, 8.43%; R$_f$ = 0.57 (hexane/toluene, 1:4). λ_{max}(DCM)/nm 242 (log ε 4.21),
20 294 inf (3.65), 305 (3.85), 358 (3.63), 467 inf (4.28), 498 (4.82). v_{max}/cm^{-1} 2953w, 2926w, 2856w, 1548s, 1510m, 1467m, 1444w, 1433w,1408m, 1371m, 1365m, 1307m, 1284w, 1224m, 1201s, 1159m, 1134w, 1078m, 1061m, 1028m, 989s, 974s, 823m. ^{1}H-NMR (500 MHz, CDCl$_3$, ppm): δ_H = 6.05 (s, 2H), 2.96-2.90 (m,
25 2H), 2.51 (s, 6H), 2.41 (s, 6H), 1.68-1.56 (m, 2H), 1.54-1.44 (m, 2H), 1.36-1.33 (m, 4H), 0.91 (t, *J* 7.0 Hz, 3H,). ^{13}C-NMR (125 MHz, CDCl$_3$): δ_C = 153.7 (s), 146.7 (s), 140.3 (s), 131.5 (s), 121.6 (d), 31.9 (t), 31.6 (t), 30.1 (t), 28.5 (t), 22.6 (t), 16.4 (q), 14.5 (q), 14.0 (q); MALDI-TOF (*m/z*): 333 (MH$^+$, 14%), 332
30 (M$^+$, 100), 331 (29).

*2,8-Dibromo-5,5-difluoro-10-hexyl-1,3,7,9-tetramethyl-5*H-*dipyrrolo[1,2-*c*:2',1'-*f*][1,3,2]diazaborinin-4-ium-5-uide* (**3**). To a stirred solution of 5,5-difluoro-10-hexyl-1,3,7,9-tetramethyl-5*H*-dipyrrolo[1,2-*c*:2',1'-*f*][1,3,2]diazaborinin-4-ium-5-uide (**2**) (1.0 g,
35 3.0 mmol) in DCM (80 mL) at *ca.* 20 °C, was added dropwise over a period of 10 min an excess of bromine (2.0 mL, 38.9 mmol). The reaction was monitored (TLC) and upon completion the mixture was allowed to cool to *ca.* 20 °C and 2M aq. Na$_2$SO$_3$ was added to the reaction mixture and the organic phase was
40 extracted with water (3 × 50 mL), dried (MgSO$_4$) and concentrated to give a dark brown solid. Column chromatography [hexane → hexane/toluene (2:8)] gave the *title compound* **3** as red needles (0.7 g; 48-50%); mp (DSC) onset: 158.4 ^{o}C, peak: 159.0 ^{o}C (MeOH); found: C, 46.66; H, 5.21; N, 5.65. C$_{19}$H$_{25}$BBr$_2$F$_2$N$_2$
45 requires C, 46.57; H, 5.14; N, 5.72%. R$_f$ = 0.86 (hexane:toluene, 1:4) . λ_{max}(DCM)/nm 242 inf (log ε 4.66), 250 (4.81), 276 (4.69), 315 inf (4.15), 372 (4.26), 493 inf (4.75), 524 (5.18). v_{max}/cm^{-1} 2959w, 2924w, 2854w, 1537s, 1467m, 1445w, 1400w, 1377w, 1350s, 1312w, 1281w, 1256w, 1246w, 1220w, 1188s, 1138m,
50 1088s, 1049m, 999s, 933w, 906w, 870w, 793m . ^{1}H-NMR (500 MHz, CDCl$_3$) δ_H = 3.00-2.96 (m, 2H), 2.57 (s, 6H), 2.44 (s, 6H), 1.68-1.46 (m, 4H), 1.36-1.33 (m, 4H), 0.91 (t, *J* 7.0 Hz, 3H); ^{13}C-NMR (125 MHz, CDCl$_3$) δ_C = 152.3 (s), 147.3 (s), 137.7 (s), 130.5 (s), 112.1 (s), 31.7 (t), 31.5 (t), 30.0 (t), 29.0 (t), 22.6 (t),
55 15.5 (q), 14.1 (q), 13.7 (q); MALDI-TOF (*m/z*): 492 (MH$^+$+3,

57%), 491 (MH$^+$+2, 39), 490 (MH$^+$+1, 100), 489 (MH$^+$, 80), 488 (M$^+$, 65), 487 (34), 486 (2).

General procedure for the Stille cross-coupling polymerization

60 To a stirred solution of the 2,6-dibromo-4-hexyl-1,3,5,7-tetramethylborondipyrromethene **3** (1 equiv.) in dry deoxygenated toluene (0.02 M) at *ca.* 20 ^{o}C was added the appropriate distannyl compound (1 equiv.), Pd$_2$dba$_3$ (0.02 equiv.) and (*o*-Tol)$_3$P (0.08 equiv.) and then this reaction mixture was heated at *ca.* 110 °C under Ar atmosphere for 24 h after which the
65 reaction mixture was allowed to cool to *ca.* 20 ^{o}C. The toluene solution was evaporated *in vacuo* and the residue was solubilized in CHCl$_3$. The polymer was purified by precipitation in MeOH, filtered and washed on Soxhlet apparatus with MeOH, hexane and CHCl$_3$. The chloroform fraction was evaporated *in vacuo* and
70 the polymer was precipitated in MeOH, filtered and finally dried under high vacuum.

Synthesis of homopolymer PB

In a predegassed round flask, were added the monomer **3** (0.25 g,
75 0.5 mmol) and toluene (14 mL) under Ar atmosphere. In a separate three-necked predegassed round flask, bis(cyclooctadiene)nickel(0) Ni(COD)$_2$ (0.32 g, 1.1 mmol) and bipyridine (0.18 g, 1.1 mmol) were added inside a glove box. The flask was removed from the glove box and 1,5-cyclooctadiene
80 (0.14 mL, 1.1 mmol) was added to the mixture. Freshly distilled DMF (8.4 mL) is added to the three necked flask and heated to *ca.* 65 ^{o}C under stirring for 30 min. To this mixture the toluene solution was added dropwise to the catalytic system and after the addition the temperature is raised to *ca.* 80 ^{o}C and the reaction is
85 kept for 72 h in the dark. The reaction mixture was worked up with conc. HCl (40 mL) and the organic layer was separated. The aqueous layer was extracted with 2 portions of DCM. The organic fractions were combined and washed with water. The solvents were removed under reduced pressure and the resulting
90 product was stirred for 30 mins in MeOH and filtered to afford a dark red product.

Acknowldgement

Notes and references

[a] *Molecular Electronics and Photonics Research Unit, Department of*
105 *Mechanical Engineering and Materials Science and Engineering, Cyprus University of Technology, 3603 Limassol, Cyprus*
* *Stelios.Choulis@cut.ac.cy*
[b] *Department of Chemistry, University of Cyprus, P.O. Box 20537, 1678 Nicosia, Cyprus*

Page 7 of 14   **RSC Advances**

c Department of Physics, Imperial College London, London SW7 2AZ, United Kingdom
d Department of Chemistry, Imperial College London, London SW7 2AZ, United Kingdom
5 *e Experimental Condensed Matter Physics Laboratory, Department of Physics, University of Cyprus, P.O. Box 20537, 1678 Nicosia, Cyprus*

15 1. G. Yu, J. Gao, J. C. Hummelen, F. Wudl and A. J. Heeger, *Science*, 1995, **270**, 1789-1791.
2. C. J. Brabec, A. Cravino, D. Meissner, N. S. Sariciftci, T. Fromherz, M. T. Rispens, L. Sanchez and J. C. Hummelen, *Adv. Funct. Mater.*, 2001, **11**, 374-380.
20 3. R. Pacios, J. Nelson, D. D. C. Bradley and C. Brabec, *Appl. Phys. Lett.*, 2003, **83**, 4764.
4. Y. Kim, S. Cook, S. M. Tuladhar, S. A. Choulis, J. Nelson, J. R. Durrant, D. D. C. Bradley, M. Giles, I. McCulloch, C.-S. Ha and M. Ree, *Nat. Mater.*, 2006, **5**, 197-203.
25 5. S. Shaheen, C. Brabec, N. Sariciftci, F. Padinger, T. Fromherz and J. Hummelen, *Appl. Phys. Lett.*, 2001, **78**, 841.
6. F. Padinger, R. S. Rittberger and N. S. Sariciftci, *Adv. Funct. Mater.*, 2003, **13**, 85-88.
7. W. Ma, C. Yang, X. Gong, K. Lee and A. J. Heeger, *Adv. Funct.*
30 *Mater.*, 2005, **15**, 1617-1622.
8. M. A. Green, K. Emery, Y. Hishikawa, W. Warta and E. D. Dunlop, *Progress in Photovoltaics: Research and Applications*, 2012, **20**, 12-20.
9. M. C. Scharber, D. Mühlbacher, M. Koppe, P. Denk, C. Waldauf, A.
35 J. Heeger and C. J. Brabec, *Adv. Mater.*, 2006, **18**, 789-794.
10. Y.-J. Cheng, S.-H. Yang and C.-S. Hsu, *Chem. Rev. (Washington, DC, U. S.)*, 2009, **109**, 5868-5923.
11. Y. Liang, Z. Xu, J. Xia, S.-T. Tsai, Y. Wu, G. Li, C. Ray and L. Yu, *Adv. Mater.*, 2010, **22**, E135-E138.
40 12. H.-Y. Chen, J. Hou, S. Zhang, Y. Liang, G. Yang, Y. Yang, L. Yu, Y. Wu and G. Li, *Nat. Photonics*, 2009, **3**, 649-653.
13. L. Huo, S. Zhang, X. Guo, F. Xu, Y. Li and J. Hou, *Angew. Chem., Int. Ed.*, 2011, **50**, 9697-9702.
14. H. Zhou, L. Yang, A. C. Stuart, S. C. Price, S. Liu and W. You,
45 *Angew. Chem., Int. Ed.*, 2011, **50**, 2995-2998.
15. S. C. Price, A. C. Stuart, L. Yang, H. Zhou and W. You, *J. Am. Chem. Soc.*, 2011, **133**, 4625-4631.
16. T.-Y. Chu, J. Lu, S. Beaupré, Y. Zhang, J.-R. m. Pouliot, S. Wakim, J. Zhou, M. Leclerc, Z. Li, J. Ding and Y. Tao, *J. Am. Chem.*
50 *Soc.*, 2011, **133**, 4250-4253.
17. C. M. Amb, S. Chen, K. R. Graham, J. Subbiah, C. E. Small, F. So and J. R. Reynolds, *J. Am. Chem. Soc.*, 2011, **133**, 10062-10065.
18. S. H. Park, A. Roy, S. Beaupre, S. Cho, N. Coates, J. S. Moon, D.
55 Moses, M. Leclerc, K. Lee and A. J. Heeger, *Nat. Photonics*, 2009, **3**, 297-302.
19. G. Ulrich, R. Ziessel and A. Harriman, *Angew. Chem., Int. Ed.*, 2008, **47**, 1184-1201.

20. A. Harriman, L. J. Mallon, K. J. Elliot, A. Haefele, G. Ulrich and R.
60 Ziessel, *J. Am. Chem. Soc.*, 2009, **131**, 13375-13386.
21. S. Zhu, N. Dorh, J. Zhang, G. Vegesna, H. Li, F.-T. Luo, A. Tiwari and H. Liu, *J. Mater. Chem.*, 2012, **22**, 2781-2790.
22. M. J. Ortiz, A. R. Agarrabeitia, G. Duran-Sampedro, J. Bañuelos Prieto, T. A. Lopez, W. A. Massad, H. A. Montejano, N. A.
65 García and I. Lopez Arbeloa, *Tetrahedron*, 2012, **68**, 1153-1162.
23. F. D'Souza, C. A. Wijesinghe, M. E. El-Khouly, J. Hudson, M. Niemi, H. Lemmetyinen, N. V. Tkachenko, M. E. Zandler and S. Fukuzumi, *Phys. Chem. Chem. Phys.*, 2011, **13**, 18168-
70 18178.
24. Y. Rio, W. Seitz, A. Gouloumis, P. Vázquez, J. L. Sessler, D. M. Guldi and T. Torres, *Chem.–Eur. J.*, 2010, **16**, 1929-1940.
25. C. Y. Lee, J. K. Jang, C. H. Kim, J. Jung, B. K. Park, J. Park, W. Choi, Y.-K. Han, T. Joo and J. T. Park, *Chem.–Eur. J.*, 2010,
75 **16**, 5586-5599.
26. C. A. Wijesinghe, M. E. El-Khouly, N. K. Subbaiyan, M. Supur, M. E. Zandler, K. Ohkubo, S. Fukuzumi and F. D'Souza, *Chem.– Eur. J.*, 2011, **17**, 3147-3156.
27. J.-Y. Liu, M. E. El-Khouly, S. Fukuzumi, D. K. Ng and P, *Chem.–
80 Asian J.*, 2011, **6**, 174-179.
28. E. Maligaspe, T. Kumpulainen, N. K. Subbaiyan, M. E. Zandler, H. Lemmetyinen, N. V. Tkachenko and F. D'Souza, *Phys. Chem. Chem. Phys.*, 2010, **12**, 7434-7444.
29. R. Ziessel, B. D. Allen, D. B. Rewinska and A. Harriman, *Chem.–
85 Eur. J.*, 2009, **15**, 7382-7393.
30. T. Lazarides, S. Kuhri, G. Charalambidis, M. K. Panda, D. M. Guldi and A. G. Coutsolelos, *Inorg. Chem.*, 2012, **51**, 4193-4204.
31. T. Rousseau, A. Cravino, E. Ripaud, P. Leriche, S. Rihn, A. De Nicola, R. Ziessel and J. Roncali, *Chem. Commun.
90 (Cambridge, U. K.)*, 2010, **46**, 5082-5084.
32. T. Bura, N. Leclerc, S. Fall, P. Lévêque, T. Heiser, P. Retailleau, S. Rihn, A. Mirloup and R. Ziessel, *J. Am. Chem. Soc.*, 2012, **134**, 17404-17407.
33. T. Mueller, R. Gresser, K. Leo and M. Riede, *Sol. Energy Mater. Sol.
95 Cells*, 2012, **99**, 176-181.
34. H.-Y. Lin, W.-C. Huang, Y.-C. Chen, H.-H. Chou, C.-Y. Hsu, J. T. Lin and H.-W. Lin, *Chem. Commun. (Cambridge, U. K.)*, 2012, **48**, 8913-8915.
35. A. Nagai, J. Miyake, K. Kokado, Y. Nagata and Y. Chujo, *J. Am.
100 Chem. Soc.*, 2008, **130**, 15276-15278.
36. C. Thivierge, A. Loudet and K. Burgess, *Macromolecules*, 2011, **44**, 4012-4015.
37. F. E. Alemdaroglu, S. C. Alexander, D. Ji, D. K. Prusty, M. Börsch and A. Herrmann, *Macromolecules*, 2009, **42**, 6529-6536.
105 38. V. R. Donuru, S. Zhu, S. Green and H. Liu, *Polymer*, 2010, **51**, 5359-5368.
39. J. C. Forgie, P. J. Skabara, I. Stibor, F. Vilela and Z. Vobecka, *Chem. Mater.*, 2009, **21**, 1784-1786.
40. B. Kim, B. Ma, V. R. Donuru, H. Liu and J. M. J. Frechet, *Chem.
110 Commun. (Cambridge, U. K.)*, 2010, **46**, 4148-4150.
41. B. C. Popere, A. M. Della Pelle and S. Thayumanavan, *Macromolecules*, 2011, **44**, 4767-4776.
42. D. Cortizo-Lacalle, C. T. Howells, S. Gambino, F. Vilela, Z. Vobecka, N. J. Findlay, A. R. Inigo, S. A. J. Thomson, P. J.

Skabara and I. D. W. Samuel, *J. Mater. Chem.*, 2012, **22**, 14119-14126.

43. A. Loudet and K. Burgess, *Chem. Rev. (Washington, DC, U. S.)*, 2007, **107**, 4891-4932.

44. J. W. G. Bloom and S. E. Wheeler, *Angew. Chem., Int. Ed.*, 2011, **50**, 7847-7849.

45. O. Inganäs, F. Zhang and M. R. Andersson, *Acc. Chem. Res.*, 2009, **42**, 1731-1739.

46. N. Blouin, A. Michaud, D. Gendron, S. Wakim, E. Blair, R. Neagu-Plesu, M. Belletête, G. Durocher, Y. Tao and M. Leclerc, *J. Am. Chem. Soc.*, 2007, **130**, 732-742.

47. F. Algı and A. Cihaner, *Organic Electronics*, 2009, **10**, 453-458.

48. V. R. Donuru, G. K. Vegesna, S. Velayudham, S. Green and H. Liu, *Chem. Mater.*, 2009, **21**, 2130-2138.

49. J. M. Frost, M. A. Faist and J. Nelson, *Adv. Mater.*, 2010, **22**, 4881-4884.

50. C. M. Cardona, W. Li, A. E. Kaifer, D. Stockdale and G. C. Bazan, *Adv. Mater.*, 2011, **23**, 2367-2371.

51. M. J. Frisch, G. W. Trucks, H. B. Schlegel, G. E. Scuseria, M. A. Robb, J. R. Cheeseman, G. Scalmani, V. Barone, B. Mennucci, G. A. Petersson, H. Nakatsuji, M. Caricato, X. Li, H. P. Hratchian, A. F. Izmaylov, J. Bloino, G. Zheng, J. L. Sonnenberg, M. Hada, M. Ehara, K. Toyota, R. Fukuda, J. Hasegawa, M. Ishida, T. Nakajima, Y. Honda, O. Kitao, H. Nakai, T. Vreven, J. Montgomery, J. A.; , J. E. Peralta, F. Ogliaro, M. Bearpark, J. J. Heyd, E. Brothers, K. N. Kudin, V. N. Staroverov, R. Kobayashi, J. Normand, K. Raghavachari, A. Rendell, J. C. Burant, S. S. Iyengar, J. Tomasi, M. Cossi, N. Rega, J. M. Millam, M. Klene, J. E. Knox, J. B. Cross, V. Bakken, C. Adamo, J. Jaramillo, R. Gomperts, R. E. Stratmann, O. Yazyev, A. J. Austin, R. Cammi, C. Pomelli, J. W. Ochterski, R. L. Martin, K. Morokuma, V. G. Zakrzewski, G. A. Voth, P. Salvador, J. J. Dannenberg, S. Dapprich, A. D. Daniels, Ö. Farkas, J. B. Foresman, J. V. Ortiz, J. Cioslowski and D. J. Fox, Gaussian 09, Revision A.1, Gaussian, Inc., Wallingford CT, 2009.

52. , Imperial college high performance computing service. http://www.imperial.ac.uk/ict/services/teachingandresearchservices/highperformancecomputing.

Table 1. Typical molecular weight characteristics for the synthesized polymers

	Mn	Mw	PDI
PB	2630	4200	1.59
PBT	1130	3220	2.85
PBTT	3710	5640	1.52
PBE	1780	2230	1.25
PBTBT	920	1400	1.52

Table 2. Optoelectronic properties of the synthesized monomers and polymers. Where available, the $E_{1/2}$ redox potentials of polymers are mentioned. If not, the peak maxima are mentioned.

| Compounds	λ_{max}^{sol} (nm)	λ_{max}^{film} (nm)	E_g^{opt} (eV)	Pl_{max}^{sol} (nm)	Pl_{max}^{film} (nm)	E^{ox} (V)	E_{HOMO} (eV)	E^{red} (V)	E_{LUMO} (eV)	E_g^{echem} (eV)
2	499	-	-	-	-					
3	525		2.25	-	-	0.74	5.61	-1.76	3.41	2.20
PB	580	577	1.97	603	690, 740			-1.63	3.77	
PBT	568	577	1.87	659	696	0.74	5.63	-1.54	3.58	2.05
PBTT	560	576	1.81	679	716	1.06, 0.68	5.66	-1.50	3.76	1.90
PBE	604	592	1.73	688	735	0.95, 0.63 (0.49)	5.61	-1.55	3.79	1.82
PBTBT	552	573	1.79	674	720	1.06, 0.73	5.67	-1.70, -1.51	3.81	1.86

Table 3. Fluorescence lifetime measurement data for the polymers **PBT** and **PBTT** and their respective blends with **PCBM**. Blend lifetimes are below the temporal instrument resolution resolution (150ps)

Sample	$A_1 = I_1/(I_1 + I_2)$ (%)	τ_1 (ps)	$A_2 = I_2/(I_1 + I_2)$ (%)	τ_2 (ps)	$\tau^* = A_1\tau_1 + A_2\tau_2$ (ps)	$\tau^{-1}, \tau_{-1}^{*-1}$ (ns^{-1})	Quench (%)
PBT	94	228	6	829	264	3.79	
PBT:PCBM	100	-	-	-			76.2
PBTT	89	217	11	742	275	3.64	
PBTT:PCBM	100	-	-	-			74.1

ARTICLE TYPE

Table 4. Quantum Chemical Calculation (QC) of polymers **PBE**, **PBT** and **PBTBT.**

Polymer	HOMO QC	LUMO QC	Eg (eV) from QC			Eg (eV) $_{opt.}$
			1st singlet	1st triplet	Singlet-Triplet ΔE	
PBE	5.118	-2.973	2.145	1.435	0.710	1.73
PBT	5.195	-2.974	2.221	1.439	0.782	1.87
PBTBT	4.997	-3.550	1.447	1.259	0.188	1.79
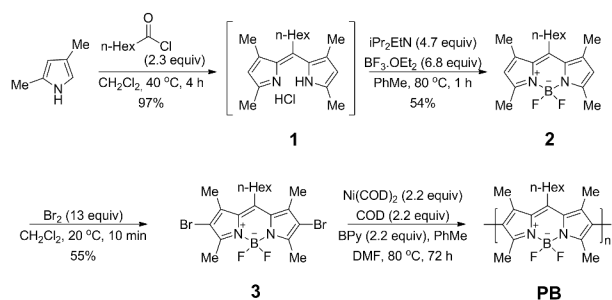
Scheme 1. Synthetic procedure for obtaining BODIPY monomer **3** and homopolymer **PB**.

5
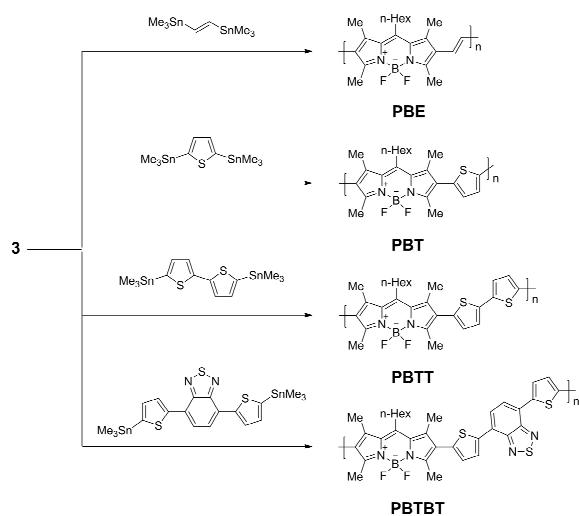
Scheme 2. Schematic representation of the synthesized copolymers based on the **BODIPY** moiety **3**. All reactions were performed in the presence of [Pd$_2$(dba)$_3$]/[(*o*-Tol)$_3$P] in PhMe at *ca.* 110 $^{\circ}$C for 1 d.
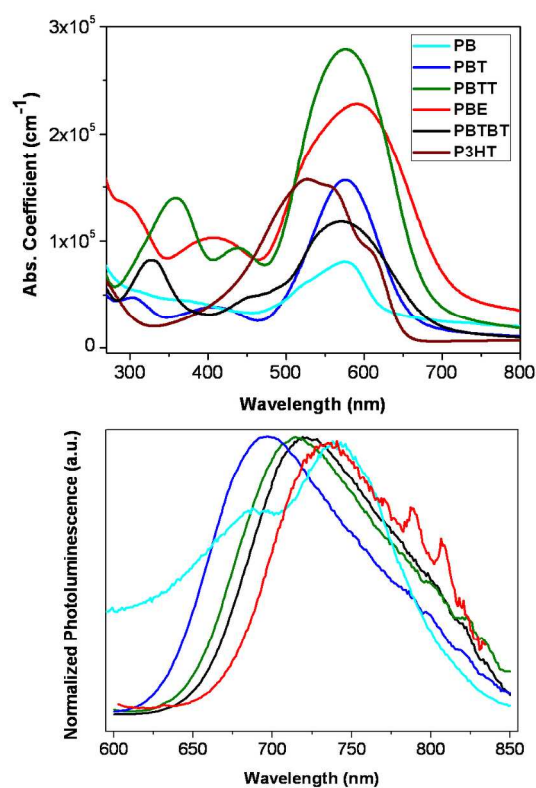
10

Figure 1. Top: Absorption spectra (top) of the polymers in thin film form. Bottom: Emission spectra of the synthesized polymers in thin film form. **PB** (cyan), **PBT** (blue), **PBTT** (green), **PBE** (red), **PBTBT** (black) and **P3HT** (brown). All films were cast from *o*-DCB solutions.
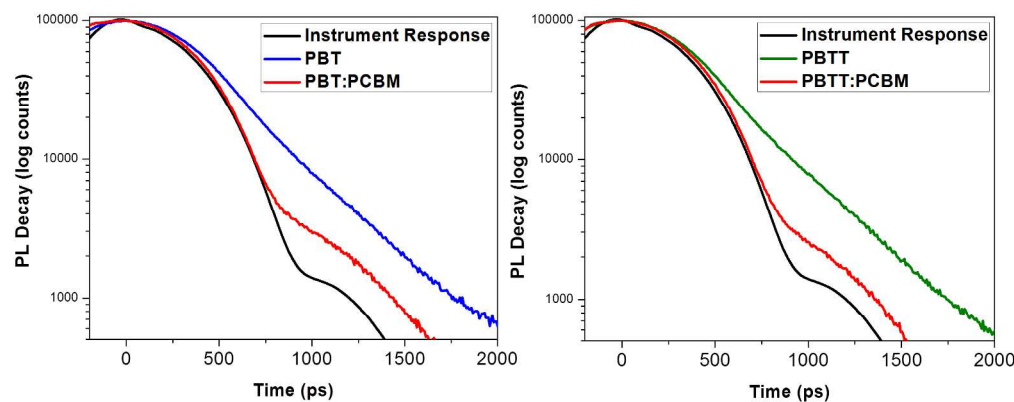
5

Figure 2. Time resolved spectra of polymers **PBT** (blue) and **PBTT** (green) in pristine thin film form and in their respective blends with **PCBM** (red lines). The instrument response is presented as well (black line).
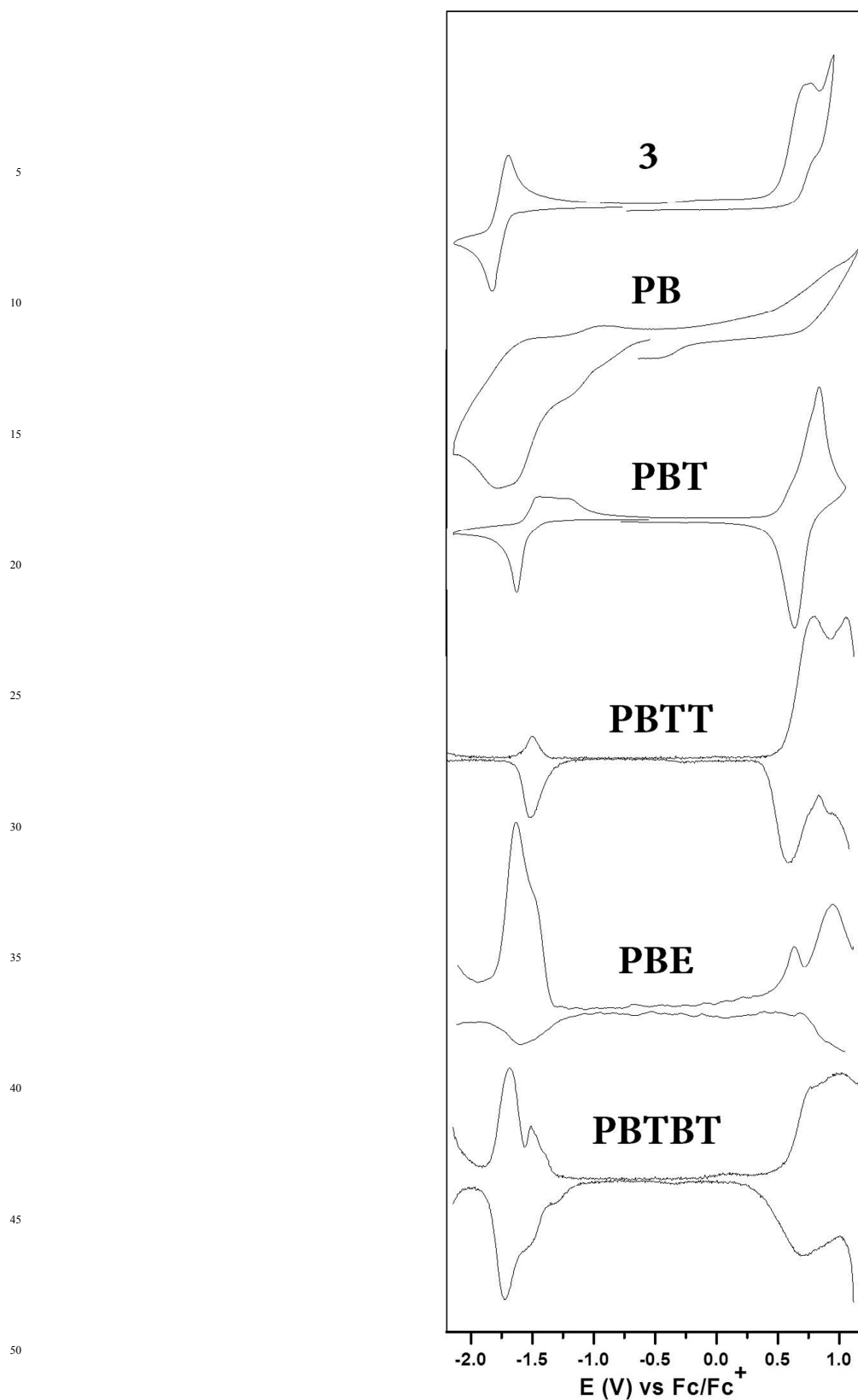
10

15

11

Figure 3. Electrochemical measurements on synthesized materials. Cyclic voltammetry (100 mV/s scan rate) on **3**, homopolymer **PB** and **PBT**. Differential Pulse Voltammetry oxidation and reductions runs, on copolymers **PBTT**, **PBE** and **PBTBT**. (Step height: 25 mV, Step Width: 5 mV, Pulse height: 50 ms, Pulse Width: 100 ms) Monomer **3** was studied in solution (0.1 M $TBAPF_6$ in DCM) and all polymers were studied in thin film (0.1 M $TBAPF_6$ in ACN). All potentials are *vs* Fc/Fc^+.
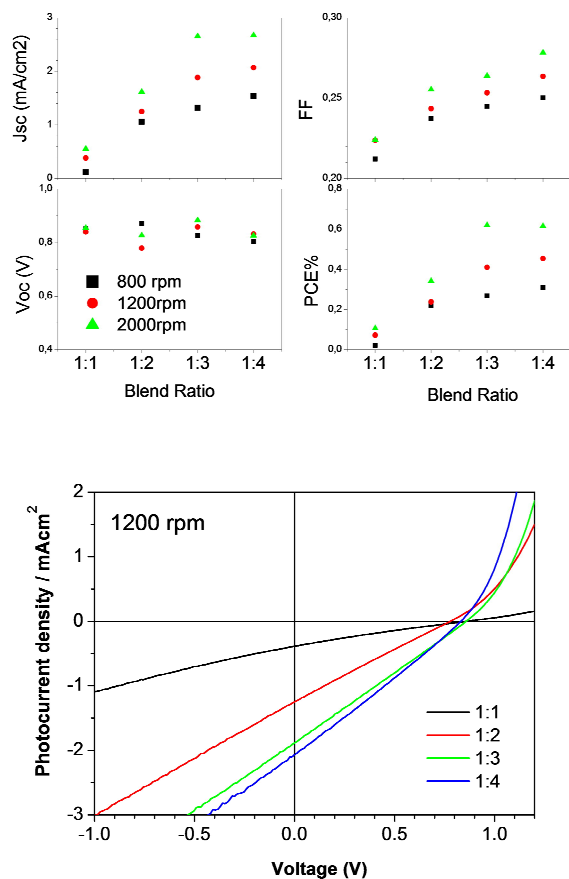
12

Figure 4. Top: Device characteristics for **PBT**:**PCBM** polymer fullerene-based solar cells under various blend ratios and film
thicknesses (spin speed). Bottom: Representative J/V curves for the 1200 rpm spin coated samples. Devices were prepared based on the
ITO/PEDOT:PSS/Blend/Ca/Al architecture.

13